Prediction of Infinite Dilution Benzene Solubility in Linear Polyethylene Melts via the Direct Particle Deletion Method

Maria Grazia De Angelis,*,† Georgios C. Boulougouris,‡,§ and Doros N. Theodorou‡

Dipartimento di Ingegneria Chimica, Mineraria e delle Tecnologie Ambientali, Università di Bologna Via Terracini, 28 40131 Bologna, Italy, Department of Materials Science and Engineering, School of Chemical Engineering, National Technical University of Athens, 9 Heroon Polytechniou Street, Zografou Campus, GR-15780 Athens, Greece, and Department of Chemical Engineering, University of Patras, Caratheodory 1, University Campus, GR-26500 Patras, Greece

Received: October 23, 2009; Revised Manuscript Received: March 27, 2010

The solubility of benzene in linear polyethylene melts was estimated via Monte Carlo simulations using a united-atom molecular model at temperatures between 373 and 573 K, in the infinite dilution limit. The excess chemical potential of the solute was evaluated with the direct particle deletion (DPD) method, whose rigorous derivation is presented here in detail: in this scheme, the benzene molecule united atoms are converted to hard spheres and then removed from the polymer system. The simulations were carried out in the N_1N_2PT ensemble using advanced Monte Carlo moves to equilibrate the polymeric phase. The evaluation of the accessible volume fraction for the "hard sphere" solute molecule required by the DPD method was performed analytically. The effect of the value of the arbitrary hard sphere diameter, d, on the computed thermodynamic quantities was determined, allowing us to establish an optimal range for the system considered. The values of Henry's law constant are in good agreement with experimental data from the literature in the temperature range considered and are comparable to those obtained with the lattice fluid and PC(SAFT) equations of state for the same system.

Introduction

The need for an accurate description of the thermodynamic properties and the phase equilibria of fluid mixtures of interest in chemical processes has stimulated an intense effort in the experimental and modeling study of such systems. In particular, great attention has been given to mixtures containing hydrocarbon macromolecules due to their immense importance in the petrochemical and polymer industries.

Traditionally, calculations concerning the phase equilibria of polymer solutions have been based on activity coefficient approaches[1−5] or equation of state (EoS) models such as the Lattice Fluid (LF),[6−8] Statistical Associating Fluid Theory (SAFT),[9−11] Perturbed-Chain SAFT (PC(SAFT)),[12,13] and Perturbed Hard Sphere Chain (PHSC) ones.[14−16]

Alternatively, one can use molecular simulations: these are based on well-defined molecular models and use few, if any, adjustable parameters. Simulations, however, require care in the choice of an efficient algorithm for sampling system configurations and of an appropriate statistical ensemble. Monte Carlo (MC) techniques are capable of sampling the highly complex configuration space of dense systems composed of large molecules and polymers more efficiently than molecular dynamics.

Examples of MC schemes that have been developed for the calculation of phase equilibria of mixtures are the Widom test particle insertion method,[17] Grand canonical MC,[18] and Gibbs Ensemble MC.[19] However, these simulation techniques fail when applied to polymers because they require insertions or transfers of molecules between phases, one of which (the polymeric one) is hard to rearrange. Several alternative techniques have been proposed for overcoming the difficulties involved in the insertions/deletions of molecules between phases.[20]

The problem of the efficient sampling of pure, long-chain polymers was solved with the introduction of the connectivity-altering end-bridging Monte Carlo move.[21,22] However, even when the polymer matrix can be fully equilibrated, the problem of inserting penetrant or solvent molecules remains. This problem is associated with the difficulty of finding "holes" of appropriate size and shape that can accommodate a large penetrant, even if special sampling MC methods, such as configurational bias, are used.

In this work, we overcome this difficulty by combining for the first time an efficient MC sampling technique for the simulation of the polymer phase with the direct particle deletion (DPD) method for evaluating the chemical potential. In the DPD scheme, the solute molecule is removed, rather than inserted, in the polymer system, to circumvent the problem of scarcity of successful insertions. In addition, the bias introduced when removing a large molecule from the polymer system that results in an improbable configuration of the polymer phase is taken into account. This method requires the estimation of the free volume accessible by a solute molecule interacting with the solvent molecules with hard-sphere repulsive interactions: this estimation can be achieved, as is the case in the present work, with an analytical procedure developed to evaluate the excluded volume of multisite molecules.[23]

In this work, the results obtained from the atomistic simulations for Henry's law constant of benzene in molten polyethylene as a function of temperature in the range of 373−573 K are compared to available experimental data and to predictions from the LF and PC(SAFT) EoS. The effect of the value of hard-sphere diameter d used in the DPD method on the excess

* Corresponding author. E-mail: grazia.deangelis@unibo.it.
† Università di Bologna Via Terracini.
‡ National Technical University of Athens.
§ University of Patras.

10.1021/jp910132j
Published on Web 04/28/2010

chemical potential and on its various contributions is evaluated and an optimal range for this parameter determined.

Background

If we consider the mixture formed by a solute (2) in a polymer (1), the calculation of sorption equilibrium can be performed by considering the polymer phase under a given temperature, pressure, and composition (isothermal−isobaric, or N_1N_2PT ensemble) and estimating the fugacity f_2 through the excess chemical potential μ_2^{ex}, which is defined as the chemical potential minus the chemical potential that the solute would have as a pure ideal gas at the same *temperature* and *molecular density* $N_2/V = \rho_{molec}x_2$, where $\rho_{molec} = (N_1 + N_2)/V$ is the total molecular density in the system and $x_2 = N_2/(N_1 + N_2)$ is the mole fraction of species 2. Note that chemical potentials here are partial molar (rather than molecular) Gibbs energies, as commonly defined in the chemical engineering literature.

$$\mu_2^{ex}(\rho_{molec}, x_2, T) = \mu_2(\rho_{molec}, x_2, T) - \mu_{2,pure}^{ig}(\rho_{molec}x_2, T) \quad (1)$$

Excess chemical potential and fugacity of the solute are related through the following equation

$$\mu_2^{ex}(\rho_{molec}x_2, T) = RT\ln\left(\frac{\beta f_2}{\rho_{molec}x_2}\right) \quad (2)$$

with $\beta = 1/(k_BT)$, $k_B = R/N_A$, and N_A is Avogadro's number.

In the limit of low pressure, the sorption thermodynamics is described completely by Henry's law constant, which can be defined based on molar (x_2, eq 3a) or mass fractions (ω_2, eq 3b)

$$H_2 \equiv \lim_{x_2\to 0}\left(\frac{f_2}{x_2}\right) \quad (3a)$$

$$H_2' \equiv \lim_{\omega_2\to 0}\left(\frac{f_2}{\omega_2}\right) \quad (3b)$$

From eqs 2 and 3b, the mass-fraction-based Henry's law constant can be expressed in terms of the excess chemical potential evaluated at infinite dilution

$$H_2' = \frac{\rho RT}{M_2}\lim_{x_2\to 0}\left[\exp\left(\frac{\mu_2^{ex}}{RT}\right)\right] \quad (4)$$

with ρ being the mass density of the pure polymer phase and M_2 being the molar mass of the solute.

The evaluation of solubility reduces to the calculation of the chemical potential. In the Widom insertion method,[17] μ is seen as the ratio of the partition functions of two systems that differ in the presence of one additional molecule. In the case of a N_1N_2PT ensemble, such as the one we are considering, the chemical potential of the solute in the solvent can be written as

$$\frac{\mu_2}{RT} = \beta\left.\frac{\partial G}{\partial N_2}\right|_{N_1,P,T} = \beta\frac{G(N_1, N_2 + 1, P, T) - G(N_1, N_2, P, T)}{(N_2 + 1) - N_2} = -\ln\frac{Q(N_1, N_2 + 1, P, T)}{Q(N_1, N_2, P, T)} \quad (5)$$

In the above expression, the Gibbs energy of the system is expressed in terms of the isothermal−isobaric partition function $Q(N_1,N_2,P,T)$. Developing the ratio of isothermal−isobaric partition functions on the right-hand side, one can ultimately express the chemical potential as a convenient ensemble average of the Boltzmann factor of the energy of interaction "felt" by a test solute molecule inserted in the N_1N_2 molecule system. As all quantities in molecular simulation, the definition of chemical potential requires that we be in the thermodynamic limit. In our simulations, too, we are dealing with effectively $N_2\to\infty$ since we have a model system that is periodically continuous in all three directions. On the other hand, the ratio $N_2/N_1 \to 0$ in our simulations, conforming to the requirements of infinite dilution, since our polymer box is large and interactions between different images of the solute are absent.

When the size of penetrant molecules is large, estimates of excess chemical potential through Widom insertion become unreliable because accessible volume domains capable of accommodating the penetrant become very limited and the calculation of solubility relies on infrequent fluctuations of the polymer matrix that yield a hole big enough to contain the penetrant. The sampling is even poorer if specific interactions, e.g., hydrogen bonding, require a definite orientation of the penetrant with respect to functional groups on the matrix. Moreover, even if some insertions were possible, the solubility calculation would not consider the local conformational adjustment of the matrix in the proximity of an inserted particle. Therefore, "insertion" techniques become very inefficient for large or strongly interacting penetrants at low temperatures; several ways to overcome the problem have been proposed.[20]

In the *inverse Widom* methods, the excess chemical potential is evaluated by comparing the N_1N_2-molecule system to the $N_1(N_2$-1)-molecule state, obtained by removal of a solute molecule

$$\frac{\mu_2}{RT} = \beta\left.\frac{\partial G}{\partial N_2}\right|_{N_1,P,T} = \beta\frac{G(N_1, N_2, P, T) - G(N_1, N_2 - 1, P, T)}{N_2 - (N_2 - 1)} = -\ln\frac{Q(N_1, N_2, P, T)}{Q(N_1, N_2 - 1, P, T)} = -\ln\left(\frac{(N_2 - 1)!\Lambda_2^{3(N_2-1)m}}{N_2!\Lambda_2^{3N_2m}}\frac{Z(N_1, N_2, P, T)}{Z(N_1, N_2 - 1, P, T)}\right) \quad (6)$$

where m is the number of sites (atoms) constituting a solute molecule (these sites can be assumed to be of equal mass without loss of generality); Λ_2 is the thermal wavelength of such a site; and $Z(N_1,N_2,P,T)$ stands for the configurational integral in the N_1N_2PT ensemble, including all intra- and intermolecular contributions to the potential energy.

The inverse Widom scheme was introduced first by Shing and Gubbins,[24] who concluded that this method is of no practical interest for the estimation of chemical potential. The reason for the inability to calculate the chemical potential via first-order free energy perturbation using eq 6 turns out to be the fact that, after removal of a molecule from a generic system of N-molecules, the new system is not a system of N-1 molecules in one of its typical configurations but rather a system, character-

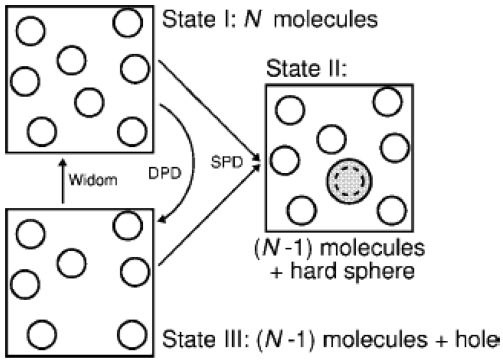

Figure 1. Schematic representation of the Widom, staged particle deletion (SPD), and direct particle deletion (DPD) methods.

ized by a very high potential energy value, of N-1 molecules and an anomalously large "hole".

This behavior is due to the fact that the configurations that are "important" for the N-molecule system, i.e., those configurations that contribute greatly to the partition function, are just a subset of the configurations important for the N-1-molecule system. In the removal of a molecule, the system samples the N-important region, while the greatest contribution lies in those N-1 important configurations outside this region: the configurations significant to the average are not sampled because of their high energy.

First attempts to improve the inverse Widom method were made by Parsonage (see refs 25−27), who proposed a modification of the intermolecular potential with the introduction of a hard core: this method led to accurate estimates of the chemical potential of Lennard-Jones fluids[27] but did not provide a clear physical justification for the adoption of a modified potential.

Kofke and Cummings[28] presented a formulation of the inverse Widom method, which calculates the free energy difference in a stepwise fashion, by considering an intermediate system that is convenient for the chemical potential calculation. Boulougouris et al.[29] developed this idea by considering the removal process as the succession of three states: (I) a system with N molecules; (II) a system with N-1 molecules and one hard sphere; and (III) a system with N-1 molecules and a hole that is the final configuration of the removal process. Such a formulation explains the use of a hard core potential without the need to alter the intermolecular potential and is referred to as the *staged particle deletion* (SPD) method (see Figure 1); its importance lies in the fact that it fixes, for the first time, clear conditions for the intermediate state.

In the SPD method, if we consider the simple case of a system of N Lennard-Jones (LJ) spheres, the ratio of configurational integrals used to evaluate the excess chemical potential is modified by introducing an intermediate system of N-1 LJ spheres and a hard sphere of diameter d. A Heaviside step function is introduced to describe the intermediate stage (II) containing the hard sphere. The expression of the chemical potential derived from this approach can be decomposed into a "volume" term (μ^{ex}_{volume}) and an "energy" term (μ^{ex}_{energy}), respectively. The first quantity is related to the accessible volume fraction for a sphere of diameter d interacting through hard sphere repulsive interactions with the other N-1 Lennard-Jones spheres. The accessible volume can be calculated numerically or, more rapidly, with an analytical scheme such as the one proposed by Dodd and Theodorou for calculating the volume of a body composed of arbitrarily configured fused spheres intersected by planes.[23] The SPD approach can be appropriately extended to the case of chain, multisite molecules composed of *multiple spheres*, with a more complicated expression for the analytical evaluation of the accessible free volume for a chain of hard spheres in a system of chains.[30]

Finally, it has to be mentioned that, in principle, the SPD method requires calculations in two different ensembles, one with N molecules and a second one with N-1 molecules. However, for simulations with a sufficiently large number of molecules, it can be safely assumed that both calculations can be performed in the same N-molecule simulation.

Direct Particle Deletion (DPD) Method. In the DPD method, presented here, it is possible to go directly from configurations of state (I) to configurations of state (III) in Figure 1. The DPD method was developed several years ago, in the context of the Ph.D. thesis of G.C. Boulougouris.[31] Although it has been successfully applied since then,[32,33] its formal derivation was never published in an international journal until last year.[34] The final expression of DPD can be considered as a generalization of the staged particle deletion method,[29] although it is based on a different thermodynamic perturbation scheme.

The deletion or insertion of a molecule can be envisioned as a transformation of a "real" molecule to an ideal gas molecule and vice versa. Both SPD and the initial Widom insertion method are based on a configuration-by-configuration comparison; i.e., in a configuration of the reference system a perturbation is performed by deleting or randomly inserting a molecule. The important aspect in this process is that since this is a first-order perturbation the molecules in the configuration are not allowed to relax from the state sampled by the reference system. In the case of inserting molecules, both perturbed and reference systems sample the same configuration space. That is, both ideal and "ghost" inserted molecules are allowed to visit all the positions in the box. In the case of the molecule removal, however, the removed molecule is not allowed to access all positions in the simulation box since it is bounded by the presence of the N-1 remaining molecules; it is only allowed to access a small part of that volume that is accessible to it. Whereas SPD introduces an intermediate state, that of N-1 molecules and one cavity, to overcome this bias, DPD proposes a novel and more drastic approach, where the perturbation is performed over all possible positions of the removed molecule, integrating over all these positions. Although the details of the DPD can now be found in the recent work of Spyriouni, Boulougouris, and Theodorou[34] along with a simple flow diagram of the method, in this work we repeat the formulation for reasons of clarity and completeness.

Equation 6 gives the total chemical potential, whereas for the purpose of solubility calculation the excess chemical potential is required. The ideal gas chemical potential of the pure solute at temperature T and molecular density $\langle N_2/V\rangle$ is given as

$$\frac{\mu_2^{ig}}{RT} = \ln\left(\left\langle\frac{N_2}{V}\right\rangle\frac{\Lambda_2^{3m}}{Z_2^{intra}}\right) \tag{7}$$

where

$$Z_2^{intra} = \int \exp[-\beta U_2^{intra}(\mathbf{q}_{(N_2)})]\mathrm{d}\mathbf{q}_{(N_2)} \tag{8}$$

is the intramolecular configurational integral; $\mathbf{q}_{(N_2)}$ is the vector of internal and orientational degrees of freedom of the N_2^{th} solute molecule; and angular brackets denote averaging in the N_1N_2PT ensemble of the solvent−solute system. If atomic Cartesian

coordinates $\mathbf{r}_i^{(N_2)}$ are used to describe the configuration of the N_2^{th} solute molecule, $\mathbf{q}_{(N_2)}$ can be defined conveniently as

$$\mathbf{q}_{(N_2)} = (\mathbf{r}_2^{(N_2)} - \mathbf{r}_1^{(N_2)}, \mathbf{r}_3^{(N_2)} - \mathbf{r}_2^{(N_2)}, ..., \mathbf{r}_m^{(N_2)} - \mathbf{r}_{m-1}^{(N_2)}) \tag{9a}$$

It is also convenient to group the degrees of freedom of solute molecules in the system in the following manner

$$\mathbf{q}_{N_2-1} \equiv (\mathbf{s}_1^{(1)}, \mathbf{r}_2^{(1)} - \mathbf{r}_1^{(1)}, ..., \mathbf{r}_m^{(1)} - \mathbf{r}_{m-1}^{(1)}, ..., \mathbf{s}_1^{(N_2-1)}, \mathbf{r}_2^{(N_2-1)} - \mathbf{r}_1^{(N_2-1)}, ..., \mathbf{r}_m^{(N_2-1)} - \mathbf{r}_{m-1}^{(N_2-1)}) \tag{9b}$$

$\mathbf{q}_{N_2\text{-}1}$ is a vector of relative coordinates that characterizes the configuration of solute molecules 1, 2, ..., N_2-1. Likewise

$$\mathbf{q}_{N_2} \equiv (\mathbf{s}_1^{(1)}, \mathbf{r}_2^{(1)} - \mathbf{r}_1^{(1)}, ..., \mathbf{r}_m^{(1)} - \mathbf{r}_{m-1}^{(1)}, ..., \mathbf{s}_1^{(N_2)}, \mathbf{r}_2^{(N_2)} - \mathbf{r}_1^{(N_2)}, ..., \mathbf{r}_m^{(N_2)} - \mathrm{r}_{m-1}^{(N_2)}) \tag{9c}$$

is a vector of relative coordinates that characterizes the configuration of solute molecules 1, 2, ..., N_2. We also introduce the vector that characterizes the configuration of the N_1 solvent molecules in the system as

$$\mathrm{q}_{N_1} \equiv (\mathbf{s}_1^{(1)}, \mathbf{r}_2^{(1)} - \mathbf{r}_1^{(1)}, ..., \mathbf{r}_l^{(1)} - \mathrm{r}_{l-1}^{(1)}, ..., \mathbf{s}_1^{(N_1)}, \mathbf{r}_2^{(N_1)} - \mathbf{r}_1^{(N_1)}, ..., \mathbf{r}_l^{(N_1)} - \mathbf{r}_{l-1}^{(N_1)}) \tag{9d}$$

where l is the number of sites of each solvent molecule. In the case of the N_1N_2PT ensemble considered here, the position vector of the first atom of each molecule (solvent or solute) has been separated and reduced ($\mathbf{s}_1^{(i)} = (\mathbf{r}_1^{(i)})/L$) with respect to the current simulation box length (L), giving rise to an integration factor (Jacobian) of V (the box volume) relative to a representation cast in terms of all atomic coordinates. Note that, based on our definitions

$$\mathbf{q}_{N_2} \equiv (\mathbf{q}_{N_2-1}, \mathbf{s}_1^{(N_2)}, \mathbf{q}_{(N_2)}) \tag{9e}$$

We also discern different contributions to the potential energy of the system: $U_2^{\text{intra}}(\mathbf{q}_{(N_2)})$ is the intramolecular potential energy of the N_2^{th} single solute molecule, considered isolated in configuration $\mathbf{q}_{(N_2)}$; $U(\mathbf{q}_{N_1},\mathbf{q}_{N_2\text{-}1})$ is the total potential energy of the system containing N_1 solvent molecules and N_2-1 solute molecules in the configuration ($\mathbf{q}_{N_1}$, $\mathbf{q}_{N_2\text{-}1}$); $U(\mathbf{q}_{N_1},\mathbf{q}_{N_2})$ is the total potential energy of the system containing N_1 solvent molecules and N_2 solute molecules in the configuration ($\mathbf{q}_{N_1}$, $\mathbf{q}_{N_2}$); and $U_{(N_2)}^{\text{inter}}(\mathbf{q}_{N_1}, \mathbf{q}_{N_2})$ is the intermolecular potential energy of interaction between the N_2^{th} solute molecule and the rest of the system (solvent and other solute molecules).

By definition

$$U_{(N_2)}^{\text{inter}}(\mathbf{q}_{N_1}, \mathbf{q}_{N_2}) = U(\mathbf{q}_{N_1}, \mathbf{q}_{N_2}) - U(\mathbf{q}_{N_1}, \mathbf{q}_{N_2-1}) - U_2^{\text{intra}}(\mathbf{q}_{(N_2)}) \tag{9f}$$

From eq 7 and the definition of the ideal gas chemical potential, we can express the excess chemical potential as

$$\frac{\mu_2^{\text{ex}}}{RT} = \frac{\mu_2}{RT} - \frac{\mu_2^{\text{ig}}}{RT} = -\ln\left(\left\langle\frac{1}{V}\right\rangle\frac{Z(N_1, N_2, P, T)}{Z(N_1, N_2 - 1, P, T)Z_2^{\text{intra}}}\right) \tag{10}$$

Since Z_2^{intra} defined by eq 8 is independent of $\mathbf{q}_{N_2\text{-}1}$, $\mathbf{q}_{N_1}$, the ratio of configurational integrals appearing in the logarithm on the right-hand side of eq 10 can be evaluated as

$$\begin{aligned} R_Z &= \frac{Z(N_1, N_2, P, T)}{Z(N_1, N_2 - 1, P, T)Z_2^{\text{intra}}} \\ &= \frac{\int \mathrm{e}^{-\beta PV}\mathrm{d}VZ(N_1, N_2, V, T)}{\int \mathrm{e}^{-\beta PV}\mathrm{d}VZ(N_1, N_2 - 1, V, T)Z_2^{\text{intra}}} \\ &= \frac{\int \mathrm{e}^{-\beta PV}V^{N_1+N_2}\mathrm{d}V\int \mathrm{e}^{-\beta U(\mathbf{q}_{N_1},\mathbf{q}_{N_2})}\mathrm{d}\mathbf{q}_{N_1}d\boldsymbol{q}_{N_2}}{\int \mathrm{e}^{-\beta PV}V^{N_1+N_2-1}\mathrm{d}V\int\int \mathrm{e}^{-\beta U_2^{\text{intra}}(\mathbf{q}_{(N_2)})}\mathrm{d}\mathbf{q}_{(N_2)}} \\ &\qquad \mathrm{e}^{-\beta U(\mathbf{q}_{N_1},\mathbf{q}_{N_2-1})}\mathrm{d}\mathbf{q}_{N_1}\mathrm{d}\mathbf{q}_{N_2-1} \end{aligned} \tag{11}$$

The procedure followed so far does not differ from the one adopted in traditional schemes of insertion and deletion. The difference in the DPD formulation lies in the identity that is used to transform the denominator of eq 11, which is written as follows

$$\begin{aligned} \int f(y)\mathrm{d}y &= \int \frac{\int g(x, y)\mathrm{d}x}{\int g(x, y)\mathrm{d}x}f(y)\mathrm{d}y \\ &= \int\int \frac{1}{\int g(x, y)dx}g(x, y)f(y)\mathrm{d}x\mathrm{d}y \end{aligned} \tag{12}$$

Equation 12 is well behaved for any function $g(x,y)$ for which $\int g(x,y)\mathrm{d}x$ is not zero when $f(y)$ is not zero. On the contrary, in traditional perturbation schemes (Widom-like and SPD) the derivation is based on a different identity

$$\begin{aligned} \int\int f(y)\mathrm{d}x\mathrm{d}y &= \int\int \frac{g(x, y)}{g(x, y)}f(y)\mathrm{d}x\mathrm{d}y \\ &= \int\int \frac{1}{g(x, y)}g(x, y)f(y)\mathrm{d}x\mathrm{d}y \end{aligned} \tag{13}$$

Although eqs 12 and 13 may look similar at first, they are quite different in physical meaning and, more importantly, in sampling efficiency. The reason can be easily understood if one considers the importance of the functions $f(y)$ and $g(x,y)f(y)$. In traditional perturbation schemes using eq 12, $f(y)$ represents the Boltzmann weight of the energy of one system (e.g., of the reference system in Widom's scheme), whereas $g(x,y)f(y)$ represents the Boltzmann weight of the energy of the other system (e.g., of the perturbed system). It is well-known that the sampling inefficiency of first-order perturbation schemes lies in the fact that $f(y)$ and $g(x,y)f(y)$ are nonzero in different parts of the configuration space. In simple words, the need for a particular treatment of the free energy perturbation comes from the fact that there are points in the configuration space for which the Boltzmann weight in the reference system is zero (or tends to zero), whereas the weight in the perturbed system after the first-order

perturbation is significant. The advantage of the direct particle deletion scheme over staged particle deletion, or over the Widom insertion scheme itself, lies in the fact that the comparison is not made on a configuration-by-configuration basis but rather involves the sum of the weights over an entire set of states in both reference and perturbed systems. This is actually the reason that the particle deletion can be directly applied to systems with hard core potentials. Furthermore, as in the case of the staged particle deletion scheme, in direct particle deletion the use of an analytical evaluation of the accessible volume (for arbitrarily complex solutes) gives a significant advantage over other free energy methods since the accessible volume part of the configuration space of the "ghost" molecule contains most of the source of uncertainty in the estimation of the chemical potential. Note that the statistical weights of both the reference and the perturbed system may be considered to have a theoretical positive value in all configuration space; in practice, however, importance sampling in statistical mechanics recognizes that only for a very small part of phase space will the values of these weights significantly differ from zero.

One can obtain different particle deletion schemes by varying the functional form of $\int g(x,y)\mathrm{d}x$. In the methodology presented here, we propose a scheme that utilizes the possibility of calculating analytically the volume accessible to any system of fused hard spheres, which is particularly convenient for high density systems. In particular, we choose

$$\int g(x,y)\mathrm{d}x = \int H_{\mathbf{q}_{N_1},\mathbf{q}_{N_2}}(\mathbf{r}_1^{(N_2)},d)\mathrm{d}\mathbf{r}_1^{(N_2)} \tag{14}$$

where $H_{\mathbf{q}_{N_1},\mathbf{q}_{N_2}}(\mathbf{r}_1^{(N_2)}, d)$ is the product of Heaviside functions[29,30] of the distances between atomic centers i on the hard solute molecule and atomic centers j in the solvent−solute matrix configuration $(\mathbf{q}_{N_1},\mathbf{q}_{N_2\text{-}1})$, each Heaviside function switching from 0 to 1 as its argument distance goes through $d_{ij} = (d_i + d_j)/2$.

The choice made corresponds to perturbing the system over the accessible volume of the solute molecule under the conditions of fixed internal and orientational degrees of freedom. That is, for the given $\mathbf{q}_{(N_2)}$ defined by the reference configuration $(\mathbf{q}_{N_1}, \mathbf{q}_{N_2})$, we evaluate the accessible volume, within configuration $(\mathbf{q}_{N_1}, \mathbf{q}_{N_2\text{-}1})$, of a "hard solute molecule", in which each atom i of the actual N_2^{th} solute molecule is replaced by a hard sphere of diameter d_i in representing its intermolecular interactions with the rest of the system. Note that by keeping the internal and orientational degrees of freedom $\mathbf{q}_{(N_2)}$ fixed what is left is the 3 overall translational degrees of freedom of the N_2^{th} solute molecule. Therefore, the accessible volume that we define, $\int H_{\mathbf{q}_{N_1},\mathbf{q}_{N_2}}(\mathbf{r}_1^{(N_2)},d)\mathrm{d}\mathbf{r}_1^{(N_2)}$, measures the locus of points where the first atom $\mathbf{r}_1^{(N_2)}$ (or, equivalently, any reference atom) of the N_2^{th} hard solute molecule can be placed such that, given its $\mathbf{q}_{(N_2)}$ vector, there is no overlap between it and the rest of the system. The *accessible volume fraction*, i.e., the volume accessible for insertion of the first atom of the hard solute molecule in orientation and internal configuration $\mathbf{q}_{(N_2)}$ normalized by the total volume of the system, is then, by definition

$$\int H_{\mathbf{q}_{N_1},\mathbf{q}_{N_2}}(\mathbf{s}_1^{(N_2)}, d/L)\mathrm{d}\mathbf{s}_1^{(N_2)} = \int H_{\mathbf{q}_{N_1},\mathbf{q}_{N_2}}(\mathbf{r}_1^{(N_2)}, d)\mathrm{d}\mathbf{r}_1^{(N_2)}/V \tag{15}$$

In previous works, we have shown that it is possible to calculate this accessible volume analytically.[30] The analytical calculation extends the work of Dodd and Theodorou, which was able to evaluate the accessible volume for a sphere in an arbitrary configuration of fused spheres.[23] In our case, we construct m hard spheres i off of each atom j constituting the N_1 solvent and N_2-1 solute molecules, attributing a radius d_{ij} to each sphere. The total volume of the set of hard spheres generated in this way corresponds to the locus of points where insertion of the first atom of the N_2^{th} solute molecule as a hard sphere molecule will result in an overlap. The hard sphere diameters d_i attributed to each atom may either all have the same value d, as is the case of the present work, or have a value depending on the atom type. The choice of optimal values follows the same criteria as in SPD.[29−31]

Finally, with the choice made for $\int g(x,y)\mathrm{d}x$, eq 11 becomes

$$R_Z = \frac{\int \mathrm{e}^{-\beta PV} V^{N_1+N_2}\mathrm{d}V \int\int \mathrm{e}^{-\beta U(\mathbf{q}_{N_1},\mathbf{q}_{N_2})}\mathrm{d}\mathbf{q}_{N_1}\mathrm{d}\mathbf{q}_{N_2}}{\int \mathrm{e}^{-\beta PV} V^{N_1+N_2-1}\mathrm{d}V \int\int\int \frac{\int H_{\mathbf{q}_{N_1},\mathbf{q}_{N_2}}(\mathbf{r}_1^{(N_2)},d)\mathrm{d}\mathbf{r}_1^{(N_2)}}{\int H_{\mathbf{q}_{N_1},\mathbf{q}_{N_2}}(\mathbf{r}_1^{(N_2)},d)\mathrm{d}\mathbf{r}_1^{(N_2)}} \times \mathrm{e}^{-\beta U_2^{\text{intra}}(\mathbf{q}_{(N_2)})}\mathrm{d}\mathbf{q}_{(N_2)}\mathrm{e}^{-\beta U(\mathbf{q}_{N_1},\mathbf{q}_{N_2-1})}\mathrm{d}\mathbf{q}_{N_1}\mathrm{d}\mathbf{q}_{N_2-1}}$$

$$= \frac{\int \mathrm{e}^{-\beta PV} V^{N_1+N_2}\mathrm{d}V \int\int \mathrm{e}^{-\beta U(\mathbf{q}_{N_1},\mathbf{q}_{N_2})}\mathrm{d}\mathbf{q}_{N_1}\mathrm{d}\mathbf{q}_{N_2}}{\int \mathrm{e}^{-\beta PV} V^{N_1+N_2-1}\mathrm{d}V \int\int\int\int \frac{1}{\int H_{\mathbf{q}_{N_1},\mathbf{q}_{N_2}}(\mathbf{r}_1^{(N_2)},d)\mathrm{d}\mathbf{r}_1^{(N_2)}} \times H_{\mathbf{q}_{N_1},\mathbf{q}_{N_2}}(\mathbf{r}_1^{(N_2)},d)\mathrm{d}\mathbf{r}_1^{(N_2)}\mathrm{e}^{-\beta U_2^{\text{intra}}(\mathbf{q}_{(N_2)})}\mathrm{d}\mathbf{q}_{(N_2)}\mathrm{e}^{-\beta U(\mathbf{q}_{N_1},\mathbf{q}_{N_2-1})}\mathrm{d}\mathbf{q}_{N_1}\mathrm{d}\mathbf{q}_{N_2-1}} \tag{16}$$

Switching variables from $\mathbf{r}_1^{(N_2)}$ to $\mathbf{s}_1^{(N_2)}$ in the denominator

$$R_Z = \frac{\int \mathrm{e}^{-\beta PV} V^{N_1+N_2}\mathrm{d}V \int\int \mathrm{e}^{-\beta U(\mathbf{q}_{N_1},\mathbf{q}_{N_2})}\mathrm{d}\mathbf{q}_{N_1}\mathrm{d}\mathbf{q}_{N_2}}{\int \mathrm{e}^{-\beta PV} V^{N_1+N_2}\mathrm{d}V \int\int\int\int \frac{1}{V\int H_{\mathbf{q}_{N_1},\mathbf{q}_{N_2}}(\mathbf{s}_1^{(N_2)},d/L)\mathrm{d}\mathbf{s}_1^{(N_2)}} \times H_{\mathbf{q}_{N_1},\mathbf{q}_{N_2}}(\mathbf{s}_1^{(N_2)},d/L)\mathrm{d}\mathbf{s}_1^{(N_2)}\mathrm{e}^{-\beta U_2^{\text{intra}}(\mathbf{q}_{(N_2)})}\mathrm{d}\mathbf{q}_{(N_2)}\mathrm{e}^{-\beta U(\mathbf{q}_{N_1},\mathbf{q}_{N_2-1})}\mathrm{d}\mathbf{q}_{N_1}\mathrm{d}\mathbf{q}_{N_2-1}} \tag{17}$$

Recognizing that $d\mathbf{q}_{N_1}d\mathbf{q}_{N_2\text{-}1}d\mathbf{s}_1^{(N_2)}d\mathbf{q}_{(N_2)} = d\mathbf{q}_{N_1}d\mathbf{q}_{N_2}$, utilizing eq 14 for the energies, and invoking the equality $H_{\mathbf{q}_{N_1},\mathbf{q}_{N_2}}(\mathbf{s}_1^{(N_2)}, d/L) = H_{\mathbf{q}_{N_1},\mathbf{q}_{N_2}}(\mathbf{r}_1^{(N_2)}, d)$, we obtain

$$R_Z = \frac{\int \mathrm{e}^{-\beta PV} V^{N_1+N_2}\mathrm{d}V \int\int \mathrm{e}^{-\beta U(\mathbf{q}_{N_1},\mathbf{q}_{N_2})}\mathrm{d}\mathbf{q}_{N_1}\mathrm{d}\mathbf{q}_{N_2}}{\int \mathrm{e}^{-\beta PV} V^{N_1+N_2}\mathrm{d}V \int\int \frac{1}{V\int H_{\mathbf{q}_{N_1},\mathbf{q}_{N_2}}(\mathbf{s}_1^{(N_2)},d/L)\mathrm{d}\mathbf{s}_1^{(N_2)}} \times H_{\mathbf{q}_{N_1},\mathbf{q}_{N_2}}(\mathbf{r}_1^{(N_2)},d)\mathrm{e}^{+\beta U_{(N_2)}^{\text{inter}}(\mathbf{q}_{N_1},\mathbf{q}_{N_2})}\mathrm{e}^{-\beta U(\mathbf{q}_{N_1},\mathbf{q}_{N_2})}\mathrm{d}\mathbf{q}_{N_1}\mathrm{d}\mathbf{q}_{N_2}} \tag{18}$$

From eq 18 it is clear that the inverse of R_Z can be expressed as an ensemble average in the N_1N_2PT ensemble

$$R_Z = \frac{1}{\left\langle \frac{1}{\int H_{\mathbf{q}_{N_1},\mathbf{q}_{N_2}}(\mathbf{s}_1^{(N_2)}, d/L)\mathrm{d}\mathbf{s}_1^{(N_2)}} H_{\mathbf{q}_{N_1},\mathbf{q}_{N_2}}(\mathbf{r}_1^{(N_2)}, d) \frac{\exp(\beta U_{(N_2)}^{\mathrm{inter}}(\mathbf{q}_{N_1}, \mathbf{q}_{N_2}))}{V} \right\rangle} \quad (19)$$

Combining eqs 10, 11, and 19 we obtain the excess chemical potential as

$$\frac{\mu_2^{\mathrm{ex}}}{RT} = \ln\left[\left\langle\frac{1}{V}\right\rangle^{-1}\left\langle \frac{1}{\int H_{\mathbf{q}_{N_1},\mathbf{q}_{N_2}}(\mathbf{s}_1^{(N_2)}, d/L)\mathrm{d}\mathbf{s}_1^{(N_2)}} H_{\mathbf{q}_{N_1},\mathbf{q}_{N_2}}(\mathbf{r}_1^{(N_2)}, d) \times \frac{\exp(\beta U_{(N_2)}^{\mathrm{inter}}(\mathbf{q}_{N_1}, \mathbf{q}_{N_2}))}{V} \right\rangle\right] \quad (20)$$

whereas the expression for the excess chemical potential via the staged particle deletion can be seen as the sum of an energetic and a volume term[29]

$$\frac{\mu_2^{\mathrm{ex}}}{RT} = -\ln\left[\left\langle\frac{1}{V}\right\rangle\left\langle H_{\mathbf{q}_{N_1},\mathbf{q}_{N_2}}(\mathbf{r}_1^{(N_2)}, d)\frac{\exp(\beta U_{(N_2)}^{\mathrm{inter}}(\mathbf{q}_{N_1}, \mathbf{q}_{N_2}))}{V}\right\rangle^{-1}\right] - \ln[\langle \int H_{\mathbf{q}_{N_1},\mathbf{q}_{N_2}}(\mathbf{s}_1^{(N_2)}, d/L)\mathrm{d}\mathbf{s}_1^{(N_2)}\rangle] = \frac{1}{RT}\mu_{\mathrm{energy}}^{\mathrm{ex}} + \frac{1}{RT}\mu_{\mathrm{volume}}^{\mathrm{ex}} \quad (21)$$

where the energetic term is in fact the free energy of changing a hard core to a real molecule and the volume term is related to the free energy of formation of a cavity of size d.

By analogous arguments, one can prove the validity of eq 20 in the canonical ensemble; in that case, all terms involving the volume are constant and cancel out, leading to a simpler expression.

It is interesting to note that, although $U_{(N_2)}^{\mathrm{inter}}(\mathbf{q}_{N_1}, \mathbf{q}_{N_2})$ appears with a positive sign within the exponential in eqs 20 and 21, the high-energy, overlapping configurations are clipped by the presence of the term $H_{\mathbf{q}_{N_1},\mathbf{q}_{N_2}}(\mathbf{r}_1^{(N_2)}, d)$ preceding the exponential. As discussed below, the statistical efficiency of the method can be tuned by selection of the hard-sphere diameters d, and there is a relatively broad range of d for which good results are obtained.[29−31]

The expansion of the chemical potential into an energetic and a cavity formation term does not only serve for methodological purposes but also can offer physical insight into complex systems. Boulougouris et al.[32] have shown that the temperature dependence of the solubility of small hydrocarbons in water and in other solvents can be explained via the interplay of those two terms, which also accounts for the minimum observed in the solubility near room temperature.[32] They also pointed out that the weak intermolecular interaction between apolar solute and water affects indirectly the effective size of the cavity that is needed to dilute an apolar molecule in water, which is larger than that needed for a polar one.[32]

We have used eq 20 to compute the excess chemical potential of benzene from N_1N_2PT Monte Carlo simulations of a PE/benzene system in the limit of infinite dilution ($N_2 = 1$). In each configuration analyzed, the equivalent hard molecule of a "real" soft benzene molecule was constructed, according to the fixed d value assigned to the CH groups of benzene. In the case of at least one overlap between any of the six spheres of the hard solute and the spheres of the atoms constituting the surrounding polymer, a contribution of zero was entered in the averaging process, as required by the $H_{\mathbf{q}_{N_1},\mathbf{q}_{N_2}}(\mathbf{r}_1^{(N_2)}, d)$ term on the right-hand side of eq 20. If no overlap was found, we proceeded to calculate analytically[23,29,30] the accessible volume fraction $\int H_{\mathbf{q}_{N_1},\mathbf{q}_{N_2}}(\mathbf{s}_1^{(N_2)}, d/L)\,\mathrm{d}\mathbf{s}_1^{(N_2)}$ for the solute, at fixed internal geometry and orientation, within the current configuration of the PE matrix. This accessible volume fraction is guaranteed to be nonzero by the condition of no overlap at the initial position of the benzene molecule. Next we computed the intermolecular potential energy $U_{(N_2)}^{\mathrm{inter}}(\mathbf{q}_{N_1},\mathbf{q}_{N_2})$ felt by the solute due to its interactions with the PE matrix: this is the energy we would obtain upon conversion of the selected molecule into a hard solute in the current configuration. Finally, we accumulated the term in the second bracket within the logarithm on the right-hand side of eq 20 and performed averaging over all configurations.

Although there is relative freedom in the choice of the hard core diameter d which, in any case, has to be larger than the minimum distance that two atomic centers can encounter under the given conditions, in practice numerical efficiency brackets our options: too large d values make an overlap of the hard sphere analogue of the solute with the solvent very likely, and this reduces the number of configurations having a nonzero contribution to the average of eq 20 due to the $H_{\mathbf{q}_{N_1},\mathbf{q}_{N_2}}(\mathbf{r}_1^{(N_2)}, d)$ term. Too small d values would require frequent sampling of high-energy, overlapping configurations having a large contribution to $\exp(\beta U_{(N_2)}^{\mathrm{inter}}(\mathbf{q}_{N_1},\mathbf{q}_{N_2}))$, which are almost never sampled in the N_1N_2PT simulation. Thus, the algorithm will work within a window of d values. That this does indeed happen is demonstrated in our work by the existence of a plateau region in the estimated chemical potential as a function of the hard sphere diameter employed.

It has to be noted that the present procedure can be applied as well to polymer systems containing several solute molecules, formed by unlike atoms: the DPD method has indeed been tested in the case of CO_2 high-pressure sorption into a polystyrene matrix in a recently published article, where the simulation of the glassy polymeric phase was performed with molecular dynamics (MD).[34]

The power and necessity of the deletion schemes lie in the existence of configurations that have a zero weight in the reference system but, upon introducing the perturbation, have a nonzero contribution to the thermodynamics of the perturbed system (e.g., this is evident in a configuration where the "ghost" molecule overlaps with at least one of the molecules in the system). In general, this can also be caused by other reasons not related directly to excluded volume, such as strongly directional, polar interactions.[32] Furthermore, a similar effect can be caused by sampling when the configuration has a nonzero but low weight in the reference system. On the basis of the above general observations on first-order free energy perturbation schemes, one should keep in mind that bad or biased sampling in a free energy perturbation scheme can be improved/corrected with an appropriate treatment of the mapping from the reference to the perturbed configuration space for the configurational point at which the reference system has a zero or almost zero weight and the perturbed system has a nonzero value. In a recent work,[35] G.C. Boulougouris provides a generalization of the particle deletion scheme that can range from particle deletion to reinsertion scheme (where a molecule of the system is reinserted as a "ghost" molecule) and a generalized weighting function can be used to overcome "indeterminate" phase space points.

TABLE 1: Molecular Model Used for Polyethylene[22]

type of interaction	potential function	potential parameters
nonbonded	$U_{LJ}(r_{ij}) = 4\varepsilon[(\sigma_{ij}/r_{ij})^{12} - (\sigma_{ij}/r_{ij})^{6}]$	$\varepsilon_{CH3}/k_B = \varepsilon_{CH2}/k_B =$ 49.3 K $\sigma_{CH3} = \sigma_{CH2} =$ 3.94 Å
bond bending	$U_{bending}(\theta)/k_B = 1/2k_\theta(\theta - \theta_{eq})^2$	$k_\theta = 57950$ K/rad^2 $\theta_{eq} = 112°$
torsional	$U_{tors}(\phi)/k_B = \sum_{k=0}^{5} c_k \cos^k(\phi)$	$c_0 = 1116$ K, $c_1 = 1462$ K $c_2 = -1578$ K, $c_3 = -368$ K $c_4 = 3156$ K, $c_5 = -3788$ K

Molecular Modeling Details

The system studied consisted of 30 linear polyethylene chains of equal length (44 united atoms per chain) that correspond to a molecular weight of 619.19 g/mol and 1 benzene molecule, formed by 6 CH united atoms. The pressure was fixed at 1 atm, and the temperature was varied between 373 and 573 K in steps of 25 K. To check for system size effects, some simulations were carried out at 573 K in a system 8 times larger than the original one (240 polyethylene chains), by keeping the polymer chain length equal to 44 and the number of benzene molecules fixed to one, as in the smaller system. Initial configurations for each isothermal run were either chosen randomly or taken from the equilibrated structure obtained at lower temperature.

The N_1N_2PT MC simulations utilized a mix of moves. Solute displacements amounted to 0.5% of all attempted moves. For sampling polymer configurations, the MC algorithm of Pant and Theodorou[21] was used, with 44.5% of all attempted moves being rotations of polymer chains, 5% single end-bond rotations, 10% flip rotations, 35% concerted-rotation-type rebridgings, and 5% volume fluctuations. The simplicity of the system, formed by relatively short chains, did not require connectivity-altering moves[21,22,36] to reach equilibration in reasonable time. The acceptance of attempted polymer and solute moves was dictated by the standard Metropolis acceptance criteria.[18]

For polyethylene, the molecular potential model employed is the one proposed by Theodorou and co-workers and used in studies of linear PE melts. The potential function and parameters are recalled in Table 1.[22] In this model, the united atom (UA) description is invoked, in which the Lennard-Jones parameters are the same for methylene and methyl groups. The bond length for polyethylene united atoms is constrained to its average value of 1.54 Å. For intramolecular polyethylene interactions between segments separated by more than three atoms along the chain, and for all intermolecular interactions, (CH_2) groups are treated as united Lennard-Jones force centers with a diameter σ of 3.94 Å and a well-depth ε of 0.098 kcal/mol.[22] The Ryckaert−Bellemans expression is employed for the torsional potential.[37]

For pure benzene, values of the potential parameters are taken from the TraPPE united-atom force field ($\sigma_2 = 3.695$ Å and $\varepsilon_2 = 0.100344$ kcal/mol).[38] For the intermolecular interactions between benzene and polyethylene united atoms, the Lorenz−Berthelot mixing rules are used, obtaining $\sigma_{12} = 3.8175$ Å and $\varepsilon_{12} = 0.099165$ kcal/mol, where 1 stands for the CH group of benzene and 2 for the CH_2 or CH_3 group of PE.

At each temperature, the benzene−polymer system was first allowed to equilibrate with a Monte Carlo run of at least 10^8 steps. At temperatures below 400 K, longer runs of $2-3 \times 10^8$ steps were carried out to ensure complete equilibration to the system. After equilibration, at least five different runs of 0.5 to 1×10^8 steps were performed for the calculation of the excess chemical potential μ^{ex} and the energetic term of the excess chemical potential, μ^{ex}_{energy}, from which the term representative of the accessible volume, μ^{ex}_{volume}, may be calculated by subtraction. The calculation of the two chemical potential contributions was performed with different values of the reduced hard sphere diameter d/σ_{12} in the range 0.75−0.95 to establish an optimal range for this parameter.

TABLE 2: Characteristic Parameters for EoS Models

LF	T^* (K)	p^* (MPa)	ρ^* (kg/L)	ref
linear PE (HDPE)	649	425	0.904	8
benzene	523	444	0.994	8

PC(SAFT)	σ (Å)	M/m (g/mol)	ε/k_B (K)	ref
PE	4.022	38.022	252.0	13
benzene	3.648	31.685	287.35	12

Equation of State Modeling Details

To test the performance of molecular simulations in comparison with macroscopic thermodynamics models, we performed calculation of infinite dilution solubility of benzene in linear polyethylene using the Lattice Fluid (LF)[6−8] and PC(SAFT)[12,13] equations of state. The values of H_2' were obtained by direct application of eq 3b, and the pure component parameters for benzene and linear polyethylene were taken from the literature and are listed in Table 2.

As it is well-known, in such models an adjustable binary parameter, k_{12}, appears in the combining rule for the parameter representative of the binary energetic interactions between the solvent and the solute. In the LF EoS the molecules are embedded in a lattice, and the energetic parameter is given by the characteristic pressure p^*_{12}, that is, the interaction energy per unit volume. In the PC(SAFT) model the molecules are represented as chains of tangent hard spheres, and the binary interactions between unlike molecule pairs are described by ε_{12}, representing the depth of the characteristic interaction energy well between two spheres of different kinds. In both models the binary energetic parameter is estimated with a combining

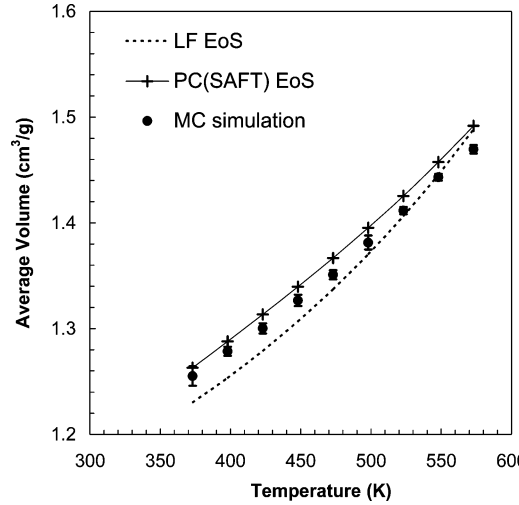

Figure 2. Specific volume of linear polyethylene at atmospheric pressure with $M_w = 619.9$ g/mol as estimated with MC simulations and LF and PC(SAFT) equations of state with parameters from Tables 1 and 2.

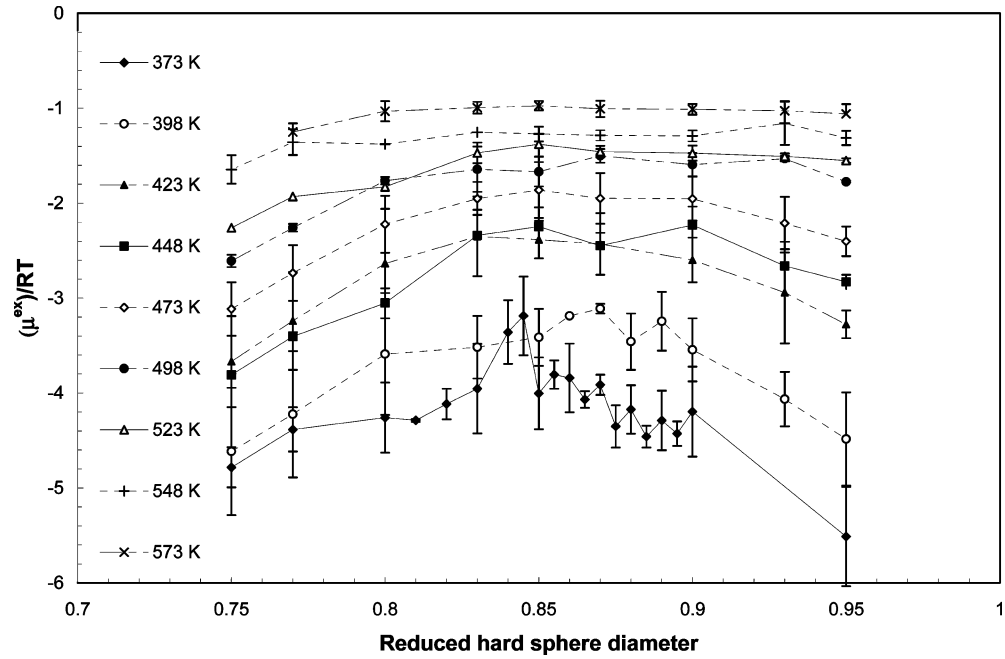

Figure 3. Values of μ^{ex}/RT for different values of hard sphere diameter at various temperatures.

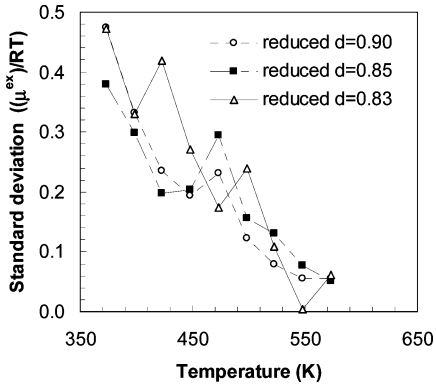

Figure 4. Values of standard deviation of the estimate of μ^{ex}/RT obtained by DPD for different values of hard sphere diameter at various temperatures. Standard deviations were obtained from the results of five independent MC runs carried out after equilibration, each of length 5×10^7 attempted steps.

rule based on the geometric mean between the corresponding pure component values

$$p^*_{12} = (1 - k_{12})\sqrt{p^*_1 p^*_2}\ (\text{LF EoS}) \qquad (22a)$$

$$\varepsilon_{12} = (1 - k_{12})\sqrt{\varepsilon_1 \varepsilon_2}\ (\text{PC(SAFT) EoS}) \qquad (22b)$$

The default value for the adjustable parameter, k_{ij}, is zero, and this approximation was used in the calculations of the infinite dilution solubility of benzene in polyethylene in this work. The solubility calculation is performed by applying the phase equilibrium condition for the solute, i.e., by equating the chemical potential of the pure solute to the chemical potential of the solute in a mixture with the solvent, for which the proper expression is provided by the LF and PC(SAFT) models. In particular, the solution of the phase equilibrium condition requires an iterative procedure for each fixed value of temperature and pressure, which includes the evaluation of the mixture density with the equation of state for the mixture. To this end, we used a fast and reliable algorithm that is implemented in a freeware software package developed by the DICMA UNIBO research group, especially built to calculate the gas/liquid solubility in polymers.[39]

Results and Discussion

Prior to performing calculations of excess chemical potential with the DPD method and comparing our predictions to the values computed with EoS models and experimental data, we compared the representation of the polymer phase obtained with the various approaches. In particular, the consistency between the present MC algorithm and the macroscopic EoS has been checked by comparing the specific volume at atmospheric pressure of linear polyethylene of molecular weight 916 g/mol, as simulated by the LF and PC(SAFT) EoS (represented by the dashed line and crosses in Figure 2, respectively) and by the present MC algorithm (represented by the filled circles in Figure 2): the macroscopic and molecular models yield similar values of the average specific volume, with a maximum discrepancy of 2%. On the other hand, it has been demonstrated in a previous paper that the MC algorithm used in this work yields a realistic representation of the experimental volumetric properties of linear PE melts.[36]

We then report the results of the evaluation of the total excess chemical potential, $(\mu^{ex})/(RT)$, and of its two main contributions that are associated with "volume" and "energetic" effects, respectively, $(\mu^{ex}_{volume})/(RT)$ and $(\mu^{ex}_{energy})/(RT)$. In a first stage we determine the effect of the value of hard segment diameter (d) on those quantities. Subsequently, the values of Henry's law constant for benzene in PE, calculated with the optimal values of d, are compared to the corresponding experimental values from the literature.

In Figure 3 we report the average values of $\mu^{ex}/(RT)$ obtained with values of hard segment diameter (d) varying from 0.75 to 0.95, at temperatures between 373 and 573 K. The error bars represent the standard deviation of the values computed on a set of at least five runs starting from different initial configurations. At lower temperatures, the standard deviation is greater, and a larger number of runs was performed. As

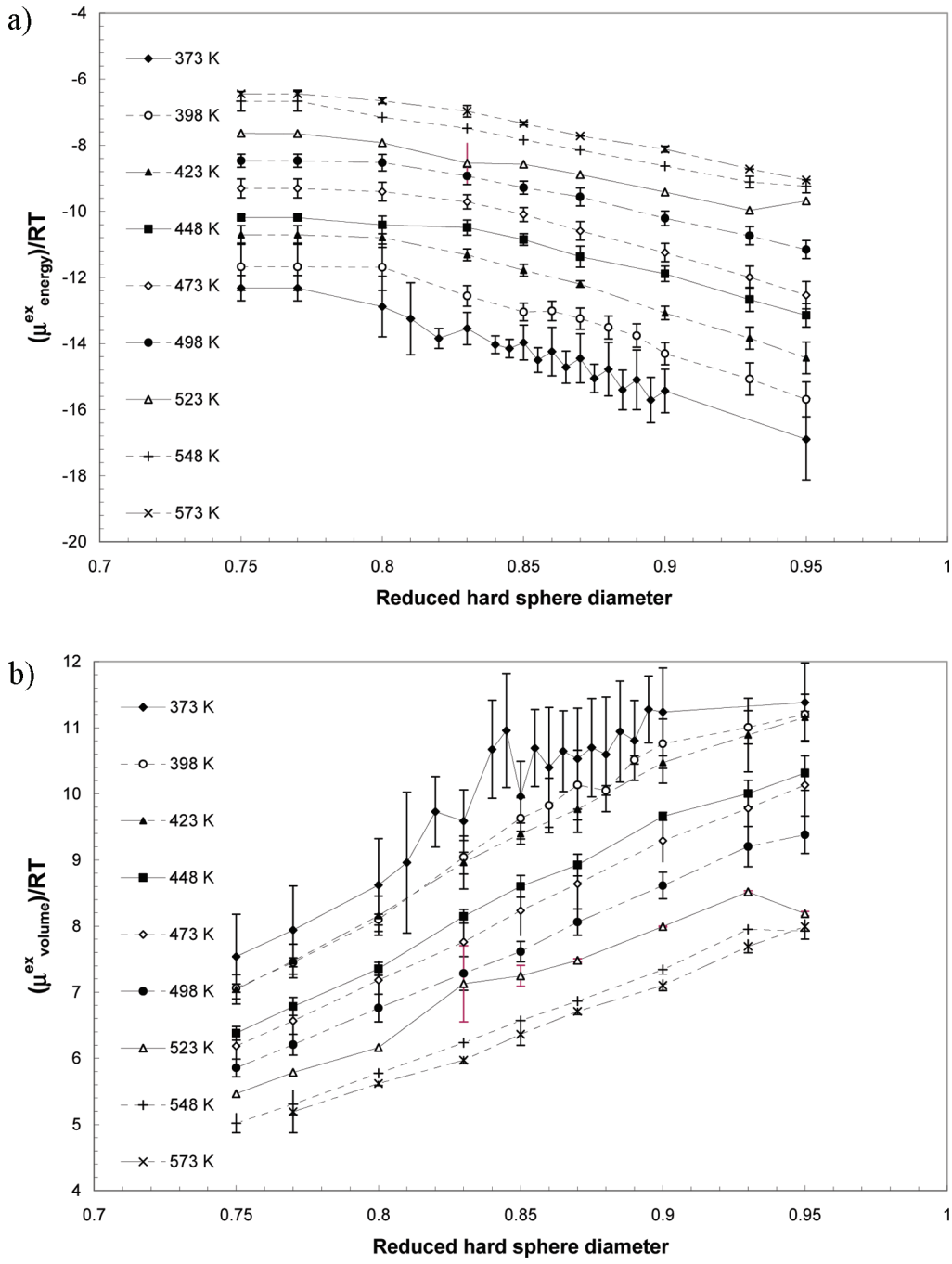

Figure 5. (a) Values of $(\mu^{ex}_{energy})/(RT)$ for different values of hard sphere diameter at various temperatures. (b) Values of $(\mu^{ex}_{volume})/(RT)$ for different values of hard sphere diameter at various temperatures.

mentioned above, in the calculations the value of d can be chosen arbitrarily as long as it is larger than the minimum distance at which two segments can be found under the conditions of interest. The attainment of a minimum value for d is accompanied by the appearance of a plateau in the plot of $(\mu^{ex}_{energy})/(RT)$ vs d: indeed, the Heaviside function that precedes the exponential term in the energetic part of chemical potential (eq 21) is always equal to one for small values of d. At the same time, selection of a relatively large value for d decreases the sampling efficiency of the free space available in the $N_1(N_2\text{-}1)$-molecule system. As a result, there is an optimal interval for the hard segment diameter that depends on the system and on the operative conditions. This optimal interval corresponds to a flat region of the curve representing $\mu^{ex}/(RT)$ vs d, which is displayed in Figure 3: within this region the value of $\mu^{ex}/(RT)$ and, therefore, of the solubility does not depend on the value of the (arbitrary) parameter d. At low temperature (373 K) the optimal interval for the reduced hard sphere diameter value lies between 0.83 and 0.90. It is interesting to notice that the flat region becomes larger with increasing temperature, and the width of the optimal interval for the hard sphere diameter value therefore becomes increasingly broader. The choice of the value of d within the optimal interval is then dictated by the necessity to improve the statistical efficiency of the method: in this respect, it has been verified that for $T < 450$ K the value of $d/\sigma_{12} = 0.85$ guarantees the smallest standard deviation of the results, while for $T > 450$ K the value of $d/\sigma_{12} = 0.90$

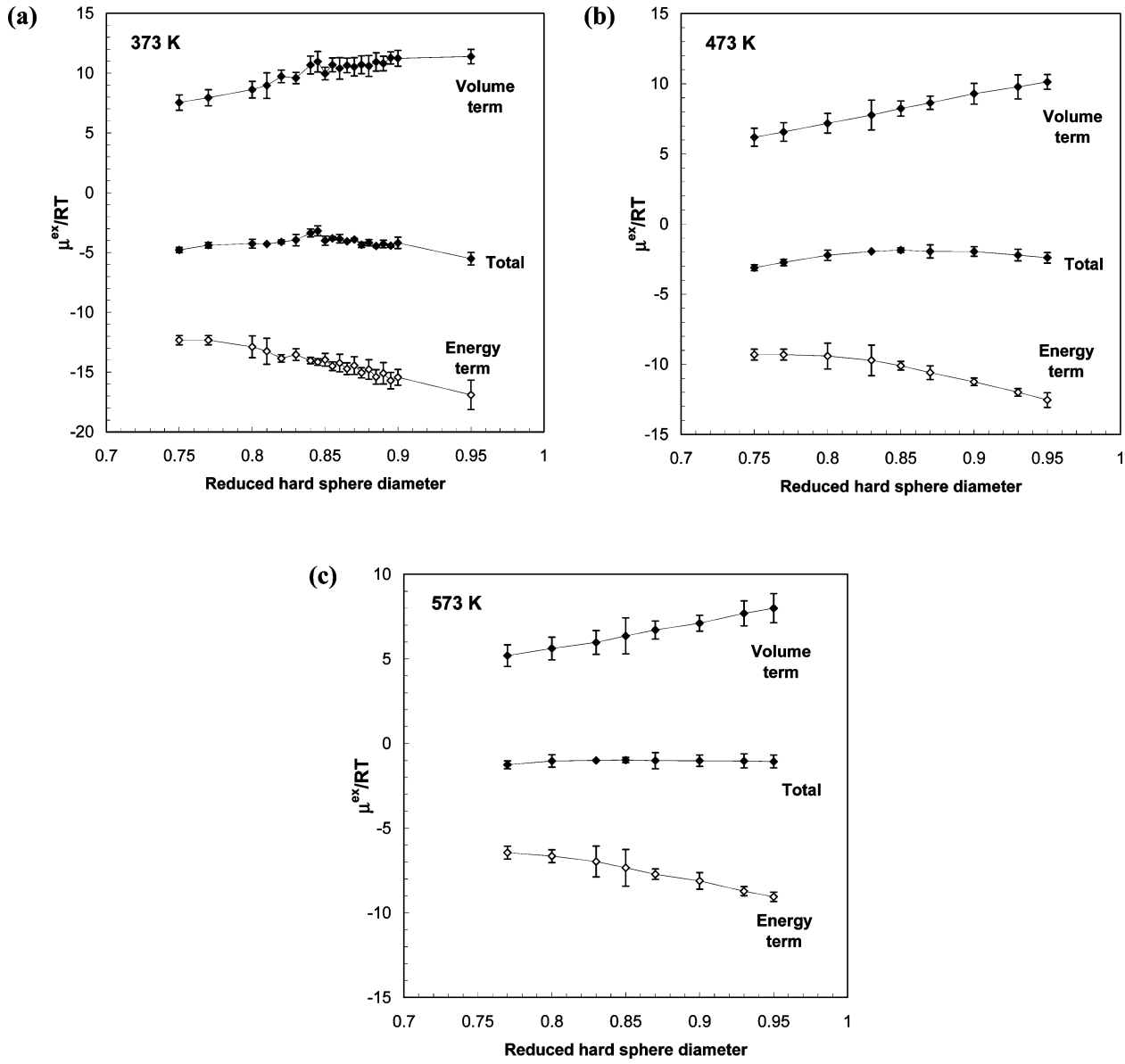

Figure 6. Values of $(\mu^{ex})/(RT)$, $(\mu^{ex}_{energy})/(RT)$, and $(\mu^{ex}_{volume})/(RT)$ for different values of hard sphere diameter at (a) 373 K, (b) 473 K, and (c) 573 K.

yields the best performance from the point of view of statistics (Figure 4). Following this analysis, the calculation of Henry's law constant and infinite dilution solubility in the system was performed with values of d/σ_{12} equal to 0.90.

By considering the energetic and volume contributions to the excess chemical potential separately (Figures 5a and 5b, respectively), one sees that the energy term increases with temperature and decreases for increasing values of reduced diameter, attaining a constant value for d/σ_{12} below 0.80: this threshold corresponds to the minimum distance between two segments, and simulations carried out with lower values of d are not meaningful in the present approach. The volume term decreases with increasing temperature and increases with the hard sphere diameter (Figure 5b). When it comes to the effect of hard sphere size, the two contributions compensate each other, so that the dependence of the excess chemical potential on the hard sphere diameter value is much slighter than that of the two contributions separately, as can be seen in Figures 6a, 6b, and 6c for the temperatures of 373, 473, and 573 K, respectively.

It has to be noticed that the energetic term is in all cases negative and decreases with increasing hard sphere size, while the volume term is positive in the range examined and increases with hard sphere diameter. The trend of the total excess chemical potential is governed by the volume term in the region of low d because the value of $(\mu^{ex}_{energy})/(RT)$ is essentially constant in this range; on the other hand, the energetic term dictates the dependence of the total chemical potential on d for values of $d/\sigma_{12} > 0.95$, as is shown for the case of 373 K in Figure 6a. In the central region, the two opposite trends cancel out, and the total excess chemical potential becomes essentially independent of d. The behavior is even more evident at 473 K (Figure 6b) and at 573 K (Figure 6c): the values of the energy and volume terms decrease and increase, respectively, with the diameter size but with an increasingly similar absolute value of slope, so that the profile of μ^{ex}/RT becomes progressively flatter with increasing temperature.

For the present analysis, it is more meaningful to present the results in terms of the infinite dilution molar solubility coefficient $S_0 = (\rho)/(M_2H'_2)$, with the mass-fraction-based

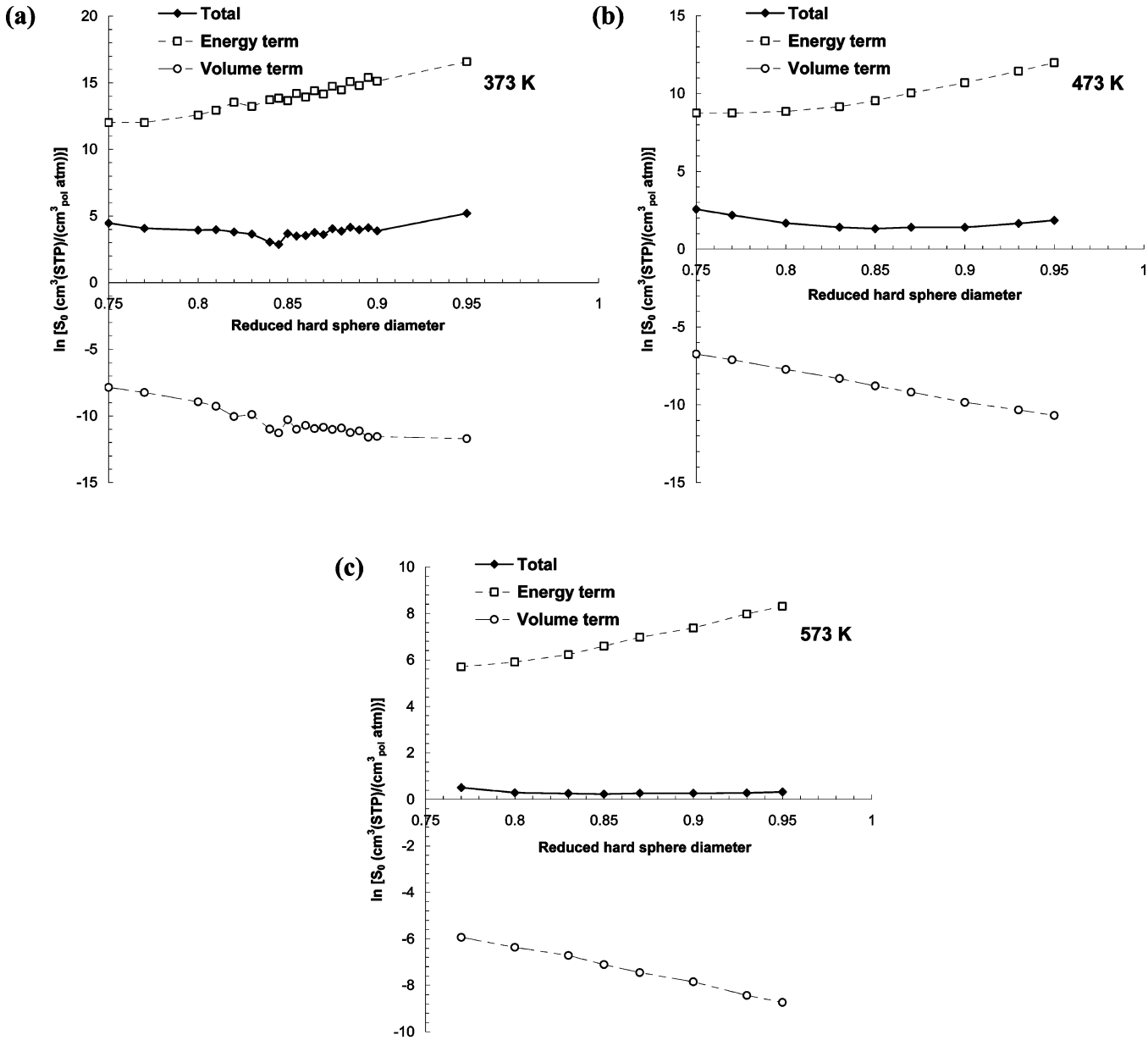

Figure 7. Values of solubility coefficient S_0 in $cm^3(STP)/(cm^3_{pol}$ atm) at (a) 373 K, (b) 473 K, and (c) 573 K as a function of d/σ_{12}, as well as energy and volume contributions to solubility.

Henry's law constant H_2' being related to the excess chemical potential through the exponential relationship of eq 4. The most common unit for S_0 is $cm^3(STP)/(cm^3_{pol}$ atm), and its value can be calculated as

$$S_0\left(\frac{\mathrm{cm}^3(\mathrm{STP})}{\mathrm{cm}^3_{\mathrm{pol}}\,\mathrm{atm}}\right) = \frac{22414}{82.1T}\exp\left(-\frac{\mu_2^{\mathrm{ex}}}{RT}\right) \qquad (23)$$

with T measured in K. The volume and energy contributions to solubility, $S_{0,\mathrm{volume}}$ and $S_{0,\mathrm{energy}}$, can be calculated by replacing the value of μ_2^{ex} in eq 23 with the value of $\mu^{\mathrm{ex}}_{\mathrm{volume}}$ and $\mu^{\mathrm{ex}}_{\mathrm{energy}}$, respectively.

The values of the logarithm of the solubility versus the reduced hard sphere diameter are reported in Figure 7. It is interesting to notice that the energetic term favors the dissolution of the solute in the polymer, while $S_{0,\mathrm{volume}}$ is lower than unity and depresses the solubility. The most significant contribution to the value of total solubility is given by the energetic term, and as a consequence, the solubility increases with increasing temperature, following the trend of the energy term. The energetic and volume terms here considered are somehow related to the enthalpic and the entropic contributions to the free energy of the system, respectively. The enthalpic and entropic contributions to the value of infinite dilution solubility S_0 can be computed explicitly for the dissolution of fluids in polymers with the macroscopic NonEquilibrium Lattice Fluid (NELF) model.[40] Indeed, the solubility at infinite dilution can be computed explicitly within this model as[40]

$$\ln\left[S_0\left(\frac{\mathrm{cm}^3(\mathrm{STP})}{\mathrm{cm}^3_{\mathrm{pol}}\,\mathrm{atm}}\right)\right] = \ln\left(\frac{T_{\mathrm{STP}}}{P_{\mathrm{STP}}T}\right) + r_2^0\left\{\left[1+\left(\frac{v_2^*}{v_1^*}-1\right)\frac{\rho_1^*}{\rho_1^0}\right]\times \ln\left(1-\frac{\rho_1^0}{\rho_1^*}\right)+\left(\frac{v_2^*}{v_1^*}-1\right)\right\} + r_2^0\left[\frac{\rho_1^0}{\rho_1^*}\frac{T_2^*}{T}\frac{2}{p_2^*}(1-k_{12})\sqrt{p_1^* p_2^*}\right] = \ln\left(\frac{T_{\mathrm{STP}}}{P_{\mathrm{STP}}T}\right)+\Phi^{(S)}+\Phi^{(H)} \qquad (24)$$

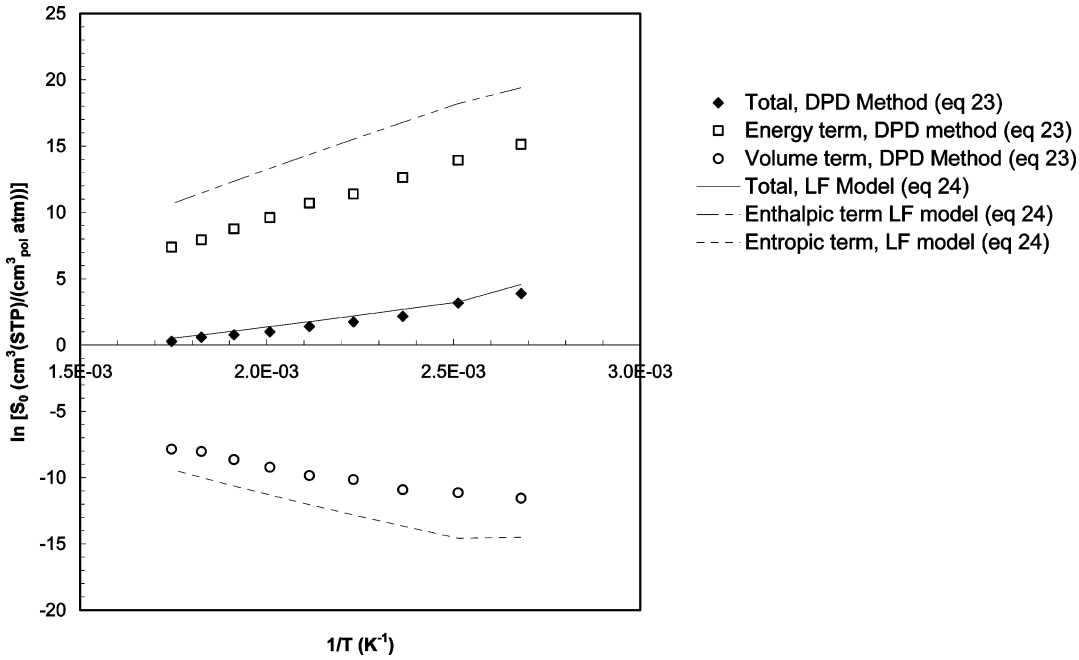

Figure 8. Values of $\ln(S_0)$ as a function of temperature, as well as energy and volume contributions to solubility as computed with the DPD method ($d/\sigma_{12} = 0.90$), using eq 23 with the energy and volume contributions to the chemical potential defined in eq 21. Values of $\ln(S_0)$ and of the enthalpic and entropic contributions $\Phi^{(H)}$ and $\Phi^{(S)}$ in eq 24 evaluated with the LF model.

where subscript 1 stands for the polymer; 2 stands for the penetrant; and the values of the various parameters come from the lattice fluid theory and they are related one another with the following relationships[6−8]

$$r_i^0 = \frac{p_i^* M_i}{RT_i^* \rho_i^*} = \frac{M_i}{\rho_i^* v_i^*} \tag{25}$$

In the LF model the enthalpic and entropic contributions to the chemical potential are clearly distinguishable, and the same conclusion is valid for the expression of solubility in eq 24. In particular, on the right-hand side of the equation the second term corresponds to the entropic contribution $\Phi^{(S)}$, while the third term is the enthalpy-related one $\Phi^{(H)}$ and the first term is a temperature-dependent constant. The above expression is entirely predictive if k_{12} is put equal to zero and contains characteristic parameters of the polymer and of the penetrant that are generally available in the literature. The same expression of S_0 can be used for both glassy and rubbery polymers, bearing in mind that the value of pure polymer density $\rho_1{}^0$ has to be provided from independent measurements if the polymer is in a nonequilibrium state, i.e., below the glass temperature T_g, while it can be computed from the LF EoS if the polymer is above T_g, as in the present case.

The enthalpic and entropic contributions to the infinite dilution solubility computed with the LF model, $\Phi^{(S)}$ and $\Phi^{(H)}$, were compared to the energy and volume contributions to S_0 evaluated with eq 23 and the DPD method for the excess chemical potential (eq 21) with a value of d/σ_{12} of 0.90 (Figure 8). The various contributions were calculated at various temperatures and compared in Figure 8. The values of S_0 evaluated with the macroscopic and the microscopic approach are rather similar; moreover, there is a parallelism between the temperature dependence of the enthalpic and entropic terms in the LF approach and that of the energy and volume term in the DPD method, showing that the various contributions in the two different approaches have a similar meaning, although they differ in absolute value.

The weight-fraction-based Henry's law constants evaluated with a reduced hard sphere diameter value of 0.90 and with eq 3b were compared to experimental data measured on polyethylene of molecular weight 159 000 and 16 600 g/mol.[41] In Figure 9 we have plotted also the values of H_2' evaluated with the LF and PC(SAFT) EoS. The average results obtained with the DPD method are extremely satisfactory and in line with the experimental values above 400 K. For lower temperatures a certain dispersion of the simulation results is observed and the experimental data are underestimated: this could be due to the fact that this temperature range is close to the melting point of polyethylene. The performance of the DPD method is also comparable to that of LF and PC(SAFT) models, represented by a dashed and a solid curve, respectively.

Finally, we checked the system size effects on the calculated solubility by performing simulations on a system 8 times larger than the original one, as specified in the modeling section. The results from the larger box are shown in Figure 9, where the average of Henry's law constant values obtained from 2 runs and with $d/\sigma_{12} = 0.90$ is reported. The comparison shows that the value obtained from the octuple system agrees with those obtained for the original system and ultimately indicates that there is no effect of the system size on the calculated quantities.

Conclusions

The solubility of benzene in linear polyethylene melts at infinite dilution was estimated in the thermal range between 373 and 573 K. The excess chemical potential of the solute was evaluated with a novel computational method (direct particle deletion) that takes origin from the staged particle deletion method proposed by Boulougouris et al. in 1999. Within this algorithm, the pseudo atoms of the solute molecule are converted to hard spheres and removed from the polymer system in one single computational step, improving the original procedure which required two subsequent mathematical operations. For

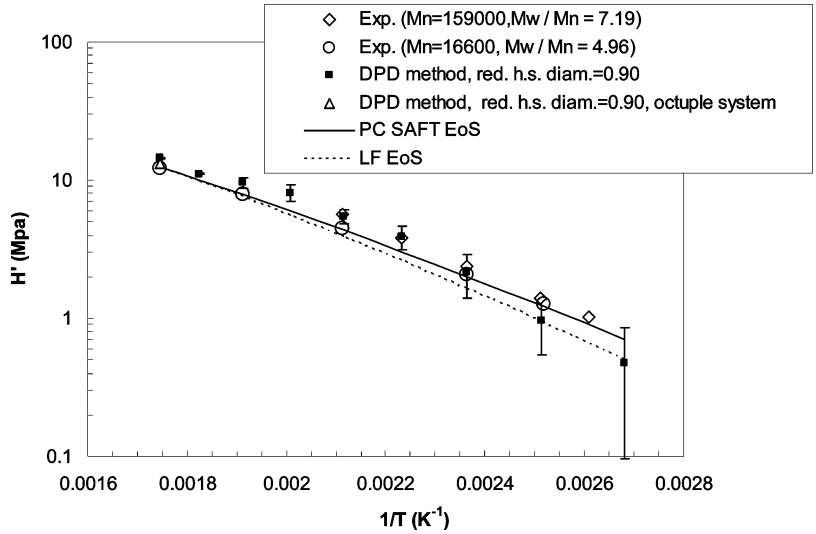

Figure 9. Values of Henry's law constants at 373−573 K. Experimental data pertain to: (1) polyethylene of $M_n = 159\,000$ g/mol, $M_w/M_n = 7.19$, data from ref 41; (2) $M_n = 16\,600$ g/mol, $M_w = 82\,300$ g/mol, $M_z = 273\,000$ g/mol, data from ref 41. Simulated data are from this work: the values obtained with the DPD method were evaluated with $d/\sigma_{12} = 0.90$, and LF and PC(SAFT) EoS results were evaluated with the characteristic parameters listed in Table 2. The triangle refers to simulations carried out in a system 8 times larger than the original one, at 573 K, with the DPD method and $d/\sigma_{12} = 0.90$.

the equilibration of the simulation box composed of 30 polyethylene chains and 1 benzene molecule, the simulation was performed in the N_1N_2PT ensemble using a fast Monte Carlo algorithm already tested on pure polyethylene melts[36] as well as the potential model for pure PE proposed by Mavrantzas et al.[22] The evaluation of the accessible volume fraction for the "hard sphere" solute molecule is performed analytically with an algorithm previously proposed[23] and appropriately modified for the case of multisite molecules.[30]

The simulations first allowed us to compute the excess chemical potential and its two contributions, that are related to energy and to free volume effects, as a function of the value chosen for the arbitrary parameter of the DPD method, i.e., the hard sphere diameter d. While the energetic term decreases with d and the volume term increases with d, the value of μ^{ex} first increases, then decreases with d, and in the range of d/σ_{12} equal to 0.83−0.90 its value is essentially constant. As a consequence, the suitable range for this parameter lies for the present system between 0.83 and 0.90, and the optimal value, chosen on the basis of statistical efficiency, was found to be equal to 0.90, which was the value used for all the calculations. The solubility at infinite dilution, S_0, can also be decomposed into an "energetic" and a "volume" term that show opposite trends with the temperature. The total solubility follows the trend of the energy term, which is greater in value. The temperature dependence of the energy and volume contribution to solubility evaluated with the present, molecular simulation method is parallel to that of the enthalpic and entropic contributions to solubility as evaluated with the macroscopic lattice fluid equation of state, testifying the entropic nature of the volume term and the enthalpic nature of the energetic term in the expression of the chemical potential of the DPD method. Finally, the values of Henry's law constant are in good agreement with experimental data from the literature for temperatures above 400 K and are comparable to those obtained with the LF and PC(SAFT) equations of state on the same system. The method has been checked for system size effects, by performing simulations in a system 8 times larger than the original one, which give results in agreement with those obtained with the smaller system.

In conclusion, it can be stated that the present method, based on the direct particle deletion method for the evaluation of excess chemical potential and on the advanced Monte Carlo algorithm for the equilibration of the polymeric melt, provides an excellent mean for predicting the solubility of medium size penetrants in polymers, when a united atom representation is used for both the penetrant and the polymer and values of the Lennard-Jones potential parameters are taken from the literature. The method requires the choice of an arbitrary hard sphere reduced diameter d/σ_{12}: the optimal range for this parameter appears to be between 0.83 and 0.90 for the present system.

Acknowledgment. M.G. De Angelis acknowledges the "Marco Polo" programme of the University of Bologna for the financial support.

References and Notes

(1) Flory, P. J. *J. Chem. Phys.* **1941**, *9*, 660.
(2) Huggins, M. L. *J. Chem. Phys.* **1941**, *9*, 440.
(3) Abrams, M. M.; Prausnitz, J. M. *AIChE J.* **1975**, *21*, 116.
(4) Oishi, T.; Prausnitz, J. M. *Ind. Eng. Chem. Res.* **1978**, *17*, 333.
(5) Elbro, H. S.; Fredenslund, A.; Rasmussen, P. *Macromolecules* **1990**, *23*, 4707.
(6) Sanchez, I. C.; Lacombe, R. H. *J. Phys. Chem.* **1976**, *80*, 2352.
(7) Lacombe, R. H.; Sanchez, I. C. *J. Phys. Chem.* **1976**, *80*, 2568.
(8) Sanchez, I. C.; Lacombe, R. H. *Macromolecules* **1978**, *11*, 1145.
(9) Chapman, W. G.; Gubbins, K. E.; Jackson, G.; Radosz, M. *Fluid Phase Equilib.* **1989**, *52*, 31.
(10) Huang, S. H.; Radosz, M. *Ind. Eng. Chem. Res.* **1990**, *29*, 2284.
(11) Chapman, W. G.; Gubbins, K. E.; Jackson, G.; Radosz, M. *Ind. Eng. Chem. Res.* **1990**, *29*, 1709.
(12) Gross, J.; Sadowski, G. *Ind. Eng. Chem. Res.* **2001**, *40*, 1244.
(13) Gross, J.; Sadowski, G. *Ind. Eng. Chem. Res.* **2002**, *41*, 1084.
(14) Song, Y.; Lambert, S. M.; Prausnitz, J. M. *Macromolecules* **1994**, *27*, 441.
(15) Song, Y.; Hino, T.; Lambert, S. M.; Prausnitz, J. M. *Fluid Phase Equilib.* **1996**, *117*, 69.
(16) Hino, T.; Prausnitz, J. M. *Fluid Phase Equilib.* **1997**, *138*, 105.
(17) Widom, B. *J. Chem. Phys.* **1963**, *39*, 2808.
(18) Allen, M. P.; Tildesley, D. J. *Computer Simulation of Liquids*; Clarendon Press: Oxford, 1987.
(19) Panagiotopoulos, A. Z.; Suter, U. W.; Reid, R. C. *Ind. Eng. Chem. Fundam.* **1986**, *25*, 525.
(20) Theodorou, D. N. Principles of molecular simulation of gas transport in polymers in material science of membranes. In *Materials Science of*

Membranes; Yampolski, Y., Pinnau, I., Freeman, B. D., Eds.; John Wiley and Sons: New York, 2006,; pp 47−92.
(21) Pant, P.V. K.; Theodorou, D. N. *Macromolecules* **1995**, *28*, 7224.
(22) Mavrantzas, V. G.; Theodorou, D. N. *Macromolecules* **1998**, *31*, 6310.
(23) Dodd, L. R.; Theodorou, D. N. *Mol. Phys.* **1991**, *72*, 1313.
(24) Shing, K. S.; Gubbins, K. E. *Mol. Phys.* **1982**, *46*, 1109.
(25) Parsonage, N. G. *J. Chem. Soc., Faraday Trans.* **1995**, *91*, 2971.
(26) Parsonage, N. G. *J. Chem. Soc., Faraday Trans.* **1996a**, *92*, 1129.
(27) Parsonage, N. G. *Mol. Phys.* **1996b**, *89*, 1133.
(28) Kofke, D. A.; Cummings, P. T. *Mol. Phys.* **1997**, *92*, 973.
(29) Boulougouris, G. C.; Economou, I. G.; Theodorou, D. N. *Mol. Phys.* **1999**, *96*, 905.
(30) Boulougouris, G. C.; Economou, I. G.; Theodorou, D. N. *J. Chem. Phys.* **2001**, *115*, 8231.
(31) Boulougouris, G. C. Ph.D. Thesis, 2001, National Technical University of Athens.
(32) Boulougouris, G. C.; Voutsas, E. C.; Economou, I. G.; Theodorou, D. N.; Tassios, D. P. *J. Phys. Chem. B* **2001**, *105*, 7792.
(33) Siegert, M. R.; Heuchel, M.; Hofmann, D. *J. Comput. Chem.* **2007**, *28*, 877.
(34) Spyriouni, T.; Boulougouris, G. C.; Theodorou, D. N. *Macromolecules* **2009**, *42*, 1759.
(35) Boulougouris, G. C. *J. Chem. Eng. Data* **2010**, accepted for publication.
(36) Karayiannis, N. Ch.; Mavrantzas, V. G.; Theodorou, D. N. *Phys. Rev. Lett.* **2002**, *88*, 105503.
(37) Ryckaert, J.-P.; Bellemans, A. *Chem. Phys. Lett.* **1975**, *30*, 123.
(38) Wick, C. D.; Martin, M. G.; Siepmann, J. I. *J. Phys. Chem. B* **2000**, *104*, 8008.
(39) Doghieri, F.; Sarti, G. C. http://serwebdicma.ing.unibo.it/polymers/index.htm.
(40) De Angelis, M. G.; Sarti, G. C.; Doghieri, F. *J. Membr. Sci.* **2007**, *289*, 109.
(41) Wohlfarth, C. Vapour-liquid equilibrium data of binary polymer solutions. *Physical Sciences Data*; Elsevier: Amsterdam, 1994; Vol. 44, Ch. 4, p 693.

JP910132J